RDR1 and SGS3, Components of RNA-Mediated Gene Silencing, Are Required for the Regulation of Cuticular Wax Biosynthesis in Developing Inflorescence Stems of Arabidopsis[1][W][OA]

Patricia Lam[2], Lifang Zhao[2], Heather E. McFarlane, Mytyl Aiga, Vivian Lam, Tanya S. Hooker, and Ljerka Kunst*

Department of Botany, University of British Columbia, Vancouver, British Columbia V6T 1Z4, Canada

The cuticle is a protective layer that coats the primary aerial surfaces of land plants and mediates plant interactions with the environment. It is synthesized by epidermal cells and is composed of a cutin polyester matrix that is embedded and covered with cuticular waxes. Recently, we have discovered a novel regulatory mechanism of cuticular wax biosynthesis that involves the ECERIFERUM7 (CER7) ribonuclease, a core subunit of the exosome. We hypothesized that at the onset of wax production, the CER7 ribonuclease degrades an mRNA specifying a repressor of *CER3*, a wax biosynthetic gene whose protein product is required for wax formation via the decarbonylation pathway. In the absence of this repressor, *CER3* is expressed, leading to wax production. To identify the putative repressor of *CER3* and to unravel the mechanism of CER7-mediated regulation of wax production, we performed a screen for suppressors of the *cer7* mutant. Our screen resulted in the isolation of components of the RNA-silencing machinery, *RNA-DEPENDENT RNA POLYMERASE1* and *SUPPRESSOR OF GENE SILENCING3*, implicating RNA silencing in the control of cuticular wax deposition during inflorescence stem development in Arabidopsis (*Arabidopsis thaliana*).

The acquisition of the cuticle, a hydrophobic structure that covers the surface of primary aerial plant tissues, represents one of the key evolutionary adaptations that allowed plants to successfully colonize land. The cuticle is synthesized by the epidermal cells and protects the plant from nonstomatal water loss (Riederer and Schreiber, 2001), UV radiation (Reicosky and Hanover, 1978), pathogen invasion (Barthlott and Neinhuis, 1997), insect attack (Eigenbrode and Espelie, 1995), and other environmental stresses (Riederer, 2006). Additionally, the cuticle has been reported to mediate osmotic stress signaling (Wang et al., 2011) and to have a role in preventing organ fusions during development by limiting the contact of neighboring epidermal cells (Sieber et al., 2000; Wang et al., 2011). The cuticle is composed of two types of lipids: cutin, a plant-specific polyester of 16- and 18-carbon-long (C16 and C18) hydroxy and epoxy fatty acids and glycerol (Nawrath, 2006; Pollard et al., 2008); and wax, a mixture of very-long-chain fatty acids (VLCFAs) and their derivatives and variable amounts of triterpenoids and phenylpropanoids (Jetter et al., 2006; Nawrath, 2006). Wax compounds that are embedded within the cutin matrix are referred to as intracuticular waxes, whereas those that coat the surface of the cutin framework are referred to as epicuticular waxes.

Cuticular wax biosynthesis takes place in several cellular compartments and involves pathways for the synthesis of VLCFA wax precursors and their subsequent modification to diverse wax constituents. C16 and C18 fatty acids are made in the plastid of epidermal cells and are then exported to the endoplasmic reticulum (ER), where they are elongated to C24 to C36 VLCFAs that serve as the precursors for wax compounds. This elongation process is catalyzed by the fatty acid elongase complex composed of four enzymes: a β-ketoacyl-CoA synthase, a β-ketoacyl-CoA reductase, a β-hydroxyacyl-CoA dehydratase, and an enoyl-CoA reductase (Millar et al., 1999; Zheng et al., 2005; Bach et al., 2008; Beaudoin et al., 2009). Following elongation, VLCFAs are processed by the enzymes of the acyl-reduction pathway, which yields primary alcohols and alkyl esters, and the decarbonylation pathway, which produces aldehydes, alkanes, secondary alcohols, and ketones (Samuels et al., 2008). The enzymes of the acyl-reduction pathway have been identified and include a fatty acyl reductase, ECERIFERUM4 (CER4), that converts VLCFA-CoAs to primary alcohols

[1] This work was supported by the Natural Sciences and Engineering Research Council of Canada (Discovery Grant to L.K., Postgraduate Scholarship to P.L., and Canada Graduate Scholarship to H.E.M.).

[2] These authors contributed equally to the article.

* Corresponding author; e-mail ljerka.kunst@ubc.ca.

The author responsible for distribution of materials integral to the findings presented in this article in accordance with the policy described in the Instructions for Authors (www.plantphysiol.org) is: Ljerka Kunst (ljerka.kunst@ubc.ca).

[W] The online version of this article contains Web-only data.

[OA] Open Access articles can be viewed online without a subscription.

www.plantphysiol.org/cgi/doi/10.1104/pp.112.199646

(Rowland et al., 2006), and a bifunctional wax synthase/diacylglycerol acyltransferase, WSD1 (Li et al., 2008), that generates wax esters. In contrast to the well-characterized acyl-reduction pathway, the only enzyme of the decarbonylation pathway with a known function is a cytochrome P450, designated MIDCHAIN ALKANE HYDROXYLASE1, responsible for the oxidation of alkanes to secondary alcohols and ketones (Greer et al., 2007). Like the VLCFA elongation enzymes, all the characterized wax modification enzymes reside in the ER (Samuels et al., 2008).

Even though a number of key wax biosynthetic enzymes and their cellular compartmentations have been established, little is known about the regulation of wax biosynthesis. The regulation of wax production is affected by both developmental and environmental cues, but only a small number of genes involved in this process have been identified to date. Recently, Wu et al. (2011) reported the isolation of the *CURLY FLAG LEAF1* (*CFL1*) gene and demonstrated that it encodes a WW domain protein involved in cuticle development in Arabidopsis (*Arabidopsis thaliana*) and rice (*Oryza sativa*). They provided biochemical evidence that AtCFL1 interacts with HDG1, a class IV homeodomain-Leu zipper transcription factor, which regulates two cuticle development-related genes, *BODYGUARD* and *FIDDLEHEAD*. Other transcription factors known to regulate cuticle formation are WAX INDUCER1/SHINE and its homologs, which primarily control cutin and indirectly wax accumulation (Aharoni et al., 2004; Broun et al., 2004; Kannangara et al., 2007). The MYB96 transcription factor was shown to promote cuticular wax biosynthesis under drought conditions by binding directly to the conserved sequences in the promoters of wax biosynthetic genes and activating their transcription (Seo et al., 2011). As well, MYB30 was shown to activate the expression of wax biosynthetic genes in response to pathogen attack, but it remains to be determined to what extent this transcription factor participates in wax biosynthesis under normal conditions (Raffaele et al., 2008).

Besides direct activation of wax biosynthetic genes by transcription factors, our work on the wax-deficient *cer7* mutant revealed that wax production in Arabidopsis stems is also controlled by the CER7 RNase, a core subunit of the exosome that is responsible for the 3′-to-5′ degradation of RNA (Hooker et al., 2007). Functional characterization of the CER7 enzyme demonstrated that it positively regulates mRNA levels of *CER3*, a wax biosynthetic gene whose protein product is required for wax formation via the decarbonylation pathway (Hooker et al., 2007; Rowland et al., 2007). Based on an analysis of *cer3* mutants, CER3 is predicted to function at the start of the decarbonylation pathway, but the reaction that it catalyzes is still unknown (Rowland et al., 2007). Because CER7 is a RNase, we proposed that it acts indirectly by degrading the mRNA specifying a repressor of *CER3* transcription. A prediction of our model is that inactivation of this putative repressor would bypass the requirement of CER7 in wax biosynthesis. Therefore, we carried out a genetic screen for mutations that suppress the stem wax deficiency of *cer7* in an attempt to identify the putative repressor as well as additional regulatory components downstream of CER7. Our screen resulted in the isolation of a series of *wax restorer* (*war*) mutants with mutations in genes distinct from *CER7*. Here, we describe the cloning and characterization of the *war3* and *war4* suppressors of *cer7*. Surprisingly, *WAR3* and *WAR4* encode components of the RNA-silencing machinery, implicating RNA silencing in the control of cuticular wax deposition during inflorescence stem development in Arabidopsis.

RESULTS

The *ProCER6*:*CER3* Transgene Complements the *cer7-3* Wax Deficiency

A key assumption in finding the target of the *CER7* exosomal RNase is that it acts on an mRNA encoding a repressor that binds the promoter of the *CER3* gene to control its transcription during development. Presumably, the mRNA of this putative repressor is not degraded in the *cer7* mutant, and the presence of the repressor inhibits *CER3* transcription. Consequently, the CER3 protein and all the wax components downstream of CER3 in the wax biosynthetic pathway are not synthesized. To test our proposed model, we attempted to rescue the *cer7* phenotype by expressing the *CER3* coding region behind the epidermis-specific *CER6* promoter (Millar et al., 1999), to which the predicted repressor should not bind. As expected, the transformants that received the *ProCER6*:*CER3* transgene were waxy (Fig. 1A) and had restored *CER3* transcript levels, as detected by quantitative real-time PCR (Fig. 1B).

As a negative control, we also introduced the *ProCER3*:*CER3* transgene into *cer7-3*, but this construct failed to complement the *cer7-3* phenotype and increased *CER3* transcript was not detected (Fig. 1B). These data provide direct evidence that the *cer7* phenotype is related to reduced *CER3* transcription and that the *CER3* promoter sequence is relevant to the CER7-mediated control of *CER3* transcript levels.

war Mutants Suppress the Wax Deficiency of *cer7*

To search for the putative *CER3* repressor and identify additional components involved in *CER7*-mediated regulation of cuticular wax biosynthesis, we performed a genetic screen for extragenic mutations that suppress the *cer7* glossy (wax-deficient) stem phenotype (Fig. 2). For the initial screen, approximately 12,000 *cer7 sti* double mutant seeds were mutagenized with ethyl methanesulfonate (M1 population). The *stichel* (*sti*) mutation, which results in a single-pronged trichome (Ilgenfritz et al., 2003), was introduced into the *cer7* background to rule out possible wild-type

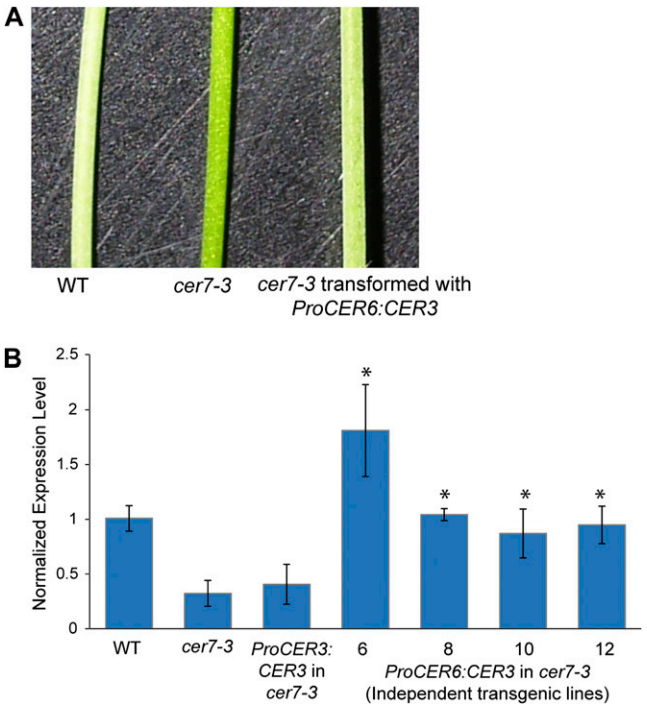

Figure 1. *CER3*, under the control of the *CER6* promoter, can complement *cer7-3*. A, Stems of 5-week-old wild type (WT; Columbia-0), *cer7-3*, and *cer7-3* transformed with the *ProCER6:CER3* transgene showing restored wax in the transgenic plant. B, Quantitative RT-PCR showing that *CER3* expression levels are restored to wild-type levels in plants carrying the *ProCER6:CER3* transgene. *ACTIN2* was used as an internal control, and control samples were normalized to 1. Values represent means ± SD ($n = 4$). Statistically significant differences from *cer7-3* ($P < 0.05$) are indicated by asterisks.

seed contamination. The M1 population was grown to maturity for bulk harvest of the M2 seeds. Visual inspection of the M2 population resulted in the identification of 824 putative *cer7* suppressors with waxy inflorescence stems. These suppressors were named *war* mutants.

The M3 progeny of all the putative suppressors were then subjected to more rigorous analyses to confirm the *sti* trichome phenotype and the presence of the original *cer7-1* mutation and to determine the wax load, wax composition, and *CER3* transcript levels of each mutant. Ninety-nine of the putative suppressor lines displayed the *sti* trichomes, and a diagnostic PCR-based cleaved-amplified polymorphic sequence assay showed that they also carried the original *cer7-1* mutant allele. Thus, the restored stem wax loads in these lines were due to mutations at sites distinct from the original *cer7-1* mutation. The 99 lines retained after the secondary screen fell into two general groups: group 1, including plants with completely waxy, wild-type-looking stems; and group 2, including plants with waxy stem bases but glossy tops. We decided to focus on suppressor lines from group 1 and selected 32 *war* lines with the highest wax loads for further analysis. Allelism tests and rough genetic mapping revealed that they fall into at least four complementation groups, *war1* through *war4* (Fig. 3).

Stem wax analyses showed that all four *war* mutants have considerably higher wax loads than the *cer7-1* mutant (Fig. 3B). *war1*, *war2*, and *war4* have 67%, 71%, and 90% of wild-type wax levels, respectively, whereas *war3* accumulates 10% greater than wild-type wax levels (Fig. 3B). Furthermore, the *cer7-1* wax composition, characterized by decreases in aldehyde, alkane, secondary alcohol, and ketone levels, was restored to near wild-type composition in the *war* lines (Fig. 3C). All the *war* mutants were also analyzed for the expression of *CER3*. Quantitative real-time PCR measurements demonstrated that *CER3* transcript accumulation was mostly or completely restored to wild-type levels and paralleled the restoration of wax loads in each suppressor line (Fig. 3D). Here, we report the cloning and characterization of genes disrupted in *war3* and *war4* mutants.

WAR3 Encodes RNA-DEPENDENT RNA POLYMERASE1

Genetic analysis of the F2 progeny from a backcross of the *war3-1 cer7-1* suppressor line to *cer7-1* showed an approximately 3:1 segregation ratio of the glossy mutant to the waxy wild type (620:232; $\chi^2 = 2.26$, $P > 0.1$), indicating that wax restoration was due to a recessive mutation in a single nuclear gene. To map the *war3-1* mutation, *war3-1 cer7-1* in the Landsberg *erecta* (L*er*) background was crossed to *cer7-3* in the Columbia-0 ecotype to create a mapping population. Thirty-five F2 plants exhibiting a waxy phenotype were used to

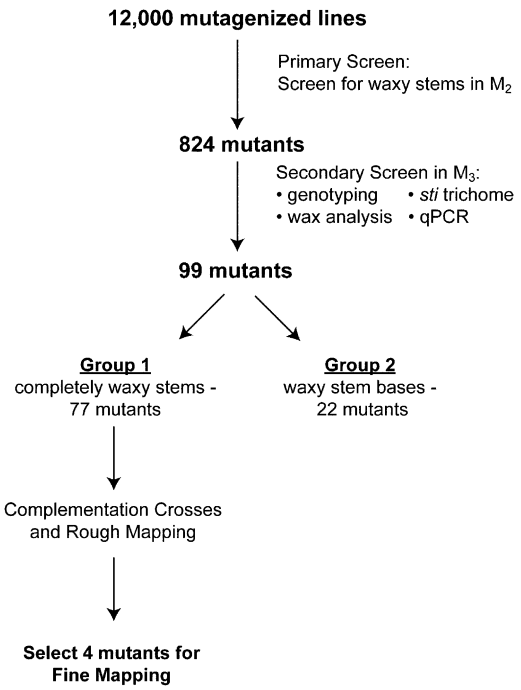

Figure 2. Summary of the suppressor screen.

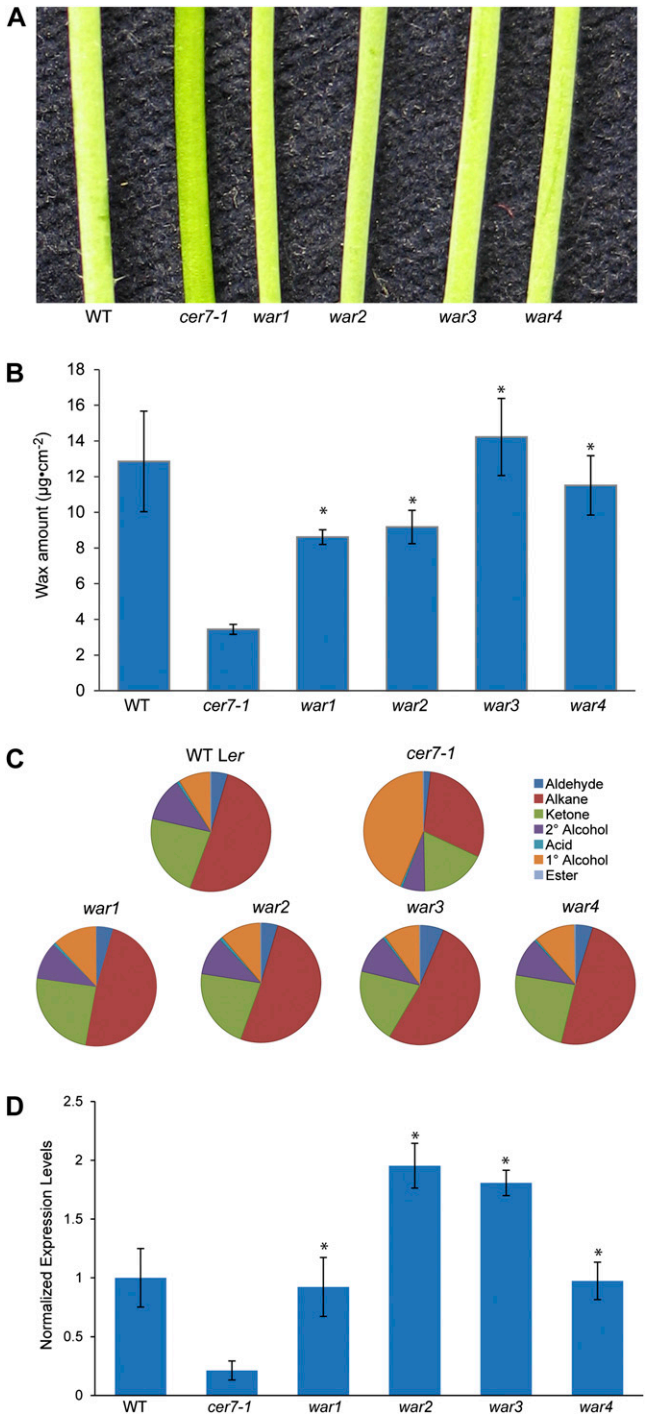

Figure 3. Analysis of *war* mutants. A, Stems of 6-week-old wild type (WT; L*er*), *cer7-1*, and four *war* mutant plants showing the suppression of the *cer7-1* wax-deficient phenotype in the *war* mutants as indicated by glaucous stems. B, Stem wax loads of *war1* to *war4* compared with the wild type and *cer7-1*. Values represent means ± SD ($n = 3$). Statistically significant differences between samples ($P < 0.05$) are indicated by asterisks. C, Stem wax composition of *war1* to *war4* compared with the wild type and *cer7-1*. Wax compositions for all *war* mutants are restored to near wild-type-like ratios of major wax components. D, Quantitative RT-PCR showing that *CER3* transcript levels are restored to wild-type levels in the *war* mutants. *ACTIN2* was used as an internal control, and control samples were normalized to 1. Values represent means ± SD ($n = 4$). Statistically significant differences between samples ($P < 0.05$) are indicated by asterisks.

establish the linkage of *war3-1* to markers F3F19 and F20D23 on chromosome 1 (Fig. 4A).

The map position of *war3-1* was further delineated to a 150-kb genomic region between markers T5E21 and F10B6I-5 using a population of 232 waxy individuals (Fig. 4A). Sequencing of several candidate genes in this region revealed a point mutation in the third exon of *At1g14790* at position 3,171 (G-to-A transition), which is predicted to cause a premature stop codon in the *war3-1* mutant. *At1g14790* was also sequenced in *war3-2* and *war3-3*, two additional alleles of *war3* found in the suppressor screen, and in both cases missense mutations were detected (Fig. 4B), confirming that *WAR3* is indeed *At1g14790*. *At1g14790* encodes RNA-DEPENDENT RNA POLYMERASE1 (RDR1; Yu et al., 2003). RDRs convert single-stranded RNA to double-stranded (ds) RNA that serves as the substrate for DICER. In Arabidopsis, there are six known RDRs. While RDR2 and RDR6 have been shown to be involved in the silencing of endogenous transcripts during development, RDR1 has not yet been demonstrated to play a role in this process (Dalmay et al., 2000; Mourrain et al., 2000; Xie et al., 2004). Instead, RDR1 has been reported to be involved in antiviral defense and shown to promote the turnover of viral RNAs in infected plants (Yu et al., 2003). Four additional alleles of *war3* were identified from the T-DNA insertional mutant collection (Alonso et al., 2003): SALK_109922, SALK_112300, SALK_125022, and SALK_007638 (Fig. 4B). Single homozygous *war3* mutants do not have a visible wax phenotype or any other morphological phenotypes. However, when homozygous *war3* T-DNA mutants were crossed into the *cer7-3* background, double mutants showed wild-type wax accumulation on inflorescence stems (Supplemental Fig. S1, A and B), indicating that these *war3* alleles were also able to suppress the *cer7*-related wax deficiency. No other morphological phenotypes were detected in the *war3 cer7* double mutants. To verify that the mutation identified in *war3* is responsible for the wax restoration of *cer7-1*, the genomic and promoter region encompassing *At1g14790* was transformed into the *war3-1 cer7-1* double mutant. Resulting transformants had wax-deficient glossy stems, confirming that *WAR3* is *RDR1* (Supplemental Fig. S2). Therefore, the *war3* alleles described here will be subsequently referred to as *rdr1* (Supplemental Table S1).

war4 Contains a Mutation in *SUPPRESSOR OF GENE SILENCING3*

The unexpected finding that *RDR1* is involved in the regulation of stem wax deposition downstream of the CER7 exoribonuclease prompted us to proceed with

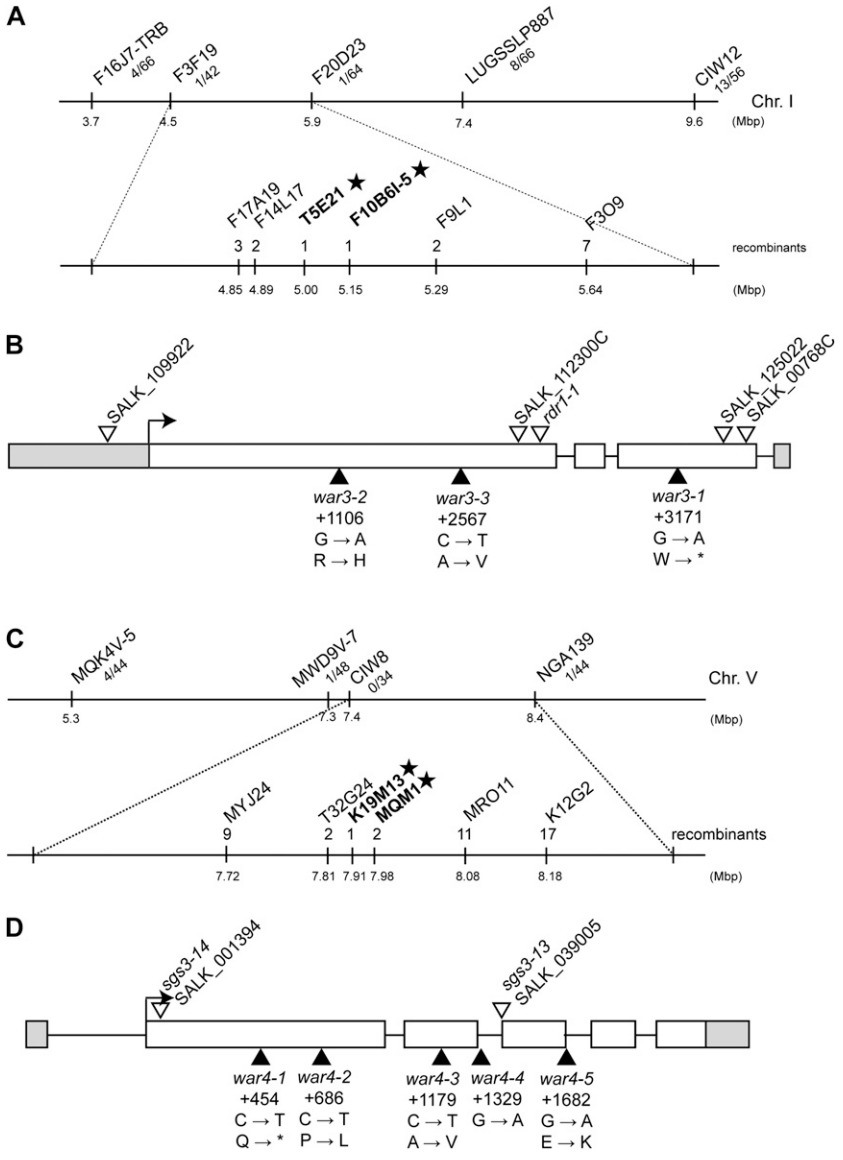

Figure 4. Positional cloning of *war3* and *war4*, and *RDR1* and *SGS3* gene structures. A, Schematic representation of the chromosomal location of *war3* as determined by fine-mapping. The markers used for mapping and the number of recombinants are indicated. B, Schematic representation of the *RDR1* gene structure. The 5′ and 3′ untranslated regions are indicated as gray boxes, exons as white boxes, and introns as black lines. The translational start site is represented by the bent arrow. The positions and types of the mutations in *rdr1* mutant alleles are also shown. C, Schematic representation of the chromosomal location of *war4* as determined by fine-mapping. The markers used for mapping and the number of recombinants are indicated. D, Schematic representation of the *SGS3* gene structure and the positions and types of mutations in *sgs3* alleles. The 5′ and 3′ untranslated regions are indicated as gray boxes, exons as white boxes, and introns as black lines. The translational start site is represented by the bent arrow.

positional cloning of additional *war* suppressors to obtain more leads about the pathway involved. Genetic analysis of the F2 progeny from a backcross of the *war4-1 cer7-1* (L*er* ecotype) suppressor line to *cer7-3* (Columbia-0 ecotype), showed an approximately 3:1 segregation ratio of the glossy mutant to the waxy wild type (1,951:641; $\chi^2 = 0.101$, $P > 0.7$), indicating that wax restoration was due to a recessive mutation in a single nuclear gene. The approximate map position of *war4* was determined using 22 F2 progeny from a *war4-1 cer7-1* cross to *cer7-3* which localized the *war4-1* mutation between markers CIW8 and NGA139 on chromosome 5 (Fig. 4C). Fine-mapping was carried out using 641 F2 plants and allowed us to narrow down the *war4-1* mutation to a 100-kb region flanked by the markers K19M13 and MQM1, which contained 22 genes. Sequencing of candidate genes in this region revealed a C-to-T point mutation at position 454 in the first exon of *At5g23570*, predicted to cause a premature stop codon. Mutations in *At5g23570* were also detected in four additional *war4* alleles (Fig. 4D). *At5g23570* encodes SUPPRESSOR OF GENE SILENCING3 (SGS3), an RNA-binding protein that is required for post-transcriptional gene silencing (Mourrain et al., 2000) and trans-acting small interfering RNA (siRNA) production (Mourrain et al., 2000; Peragine et al., 2004). SGS3 is thought to bind and protect RNA from degradation before its conversion to dsRNA by an RDR (Yoshikawa et al., 2005). We obtained two T-DNA insertional *war4* mutants from the T-DNA insertional mutant collection (Alonso et al., 2003), *sgs3-13* (SALK_039005) and *sgs3-14* (SALK_001394), which contain T-DNA insertions in the second intron and the first exon of *At5g23570*, respectively. The single *sgs3* mutants do not exhibit stem wax deficiency, but as described previously for several other *sgs3* alleles, *sgs3-13* and *sgs3-14* have slightly downward-curled leaf margins (Peragine et al., 2004). To test the ability of

sgs3-13 to suppress the *cer7*-caused stem wax deficiency like the *war4-1* allele, we crossed it into the *cer7-3* background. The resulting double mutant showed a waxy wild-type stem phenotype (Supplemental Fig. S1, A and B) and downward-curled leaf margins, further demonstrating that *At5g23570* is *WAR4*. In addition, we introduced the *SGS3* coding region under the control of the cauliflower mosaic virus 35S promoter into the *war4-1 cer7-1* double mutant and obtained glossy *cer7*-like T1 progeny, indicative of successful complementation (Supplemental Fig. S2). Thus, *WAR4* is *SGS3*, and we renamed all the *war4* alleles described here *sgs3* (Fig. 4D; Supplemental Table S2).

RDR1 and *SGS3* Are Expressed throughout the Plant

Quantitative reverse transcription (RT)-PCR was used to assess the expression levels of *RDR1* and *SGS3* in various organs. Aerial tissues were harvested from 4- to 6-week-old plants, whereas seedlings and roots were collected from 14-d-old plants. *RDR1* and *SGS3* expression was detected in all tissues (Fig. 5), but at varying levels. Expression patterns for *RDR1* and *SGS3* were very similar, with high expression levels found in seedlings, cauline leaves, rosette leaves, and flowers. Moderate levels were detected in the stem top and base. Low levels of *RDR1* and *SGS3* expression were detected in roots and siliques.

To determine cell type-specific expression patterns of *RDR1* and *SGS3*, we examined GUS activity in transgenic plants transformed with constructs in which the promoter region of *RDR1* or *SGS3* was fused to the *GUS* reporter gene (*ProRDR1*:*GUS* or *ProSGS3*:*GUS*, respectively). Cross-sections of the top of the stem show that both *ProRDR1*:*GUS* and *ProSGS3*:*GUS* are expressed in all stem tissues (Fig. 6, A and B).

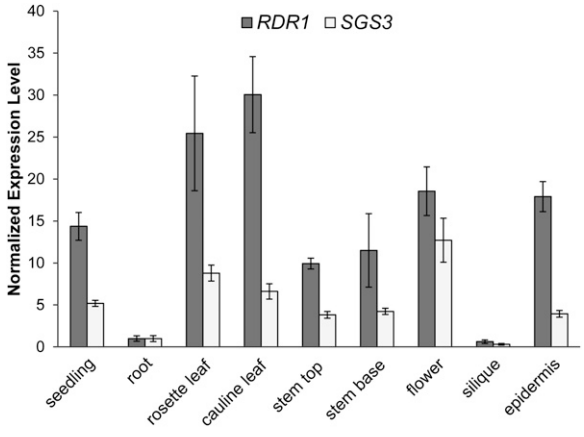

Figure 5. Expression analysis of *RDR1* and *SGS3* in different organs and tissues of wild-type Arabidopsis (Columbia-0) as determined by quantitative RT-PCR. *ACTIN2* was used as an internal control, and control samples were normalized to 1. Values represent means ± SD ($n = 4$).

In order to establish the subcellular localization of SGS3, an SGS3:yellow fluorescent protein (YFP) fusion protein under the control of the 35S promoter was created (*Pro35S*:*SGS3*:*YFP*) and expressed in transgenic *sgs3-15 cer7-1* plants. The *SGS3*:*YFP* transgene was able to complement the waxy phenotype of *sgs3-15 cer7-1*, indicating that the SGS3:YFP fusion protein was functional. In developing stems, SGS3 was found to be localized to a reticulate structure typical of the ER (Fig. 6C; Supplemental Fig. S3, A–C). When leaves were examined, in addition to localization to the ER, SGS3 was also found to be present in the cytoplasm and in punctate structures, also termed cytoplasmic foci or granules, in agreement with previous reports (Fig. 6D; Supplemental Fig. S3, D–F; Glick et al., 2008; Elmayan et al., 2009; Kumakura et al., 2009). The punctae observed were not motile, suggesting that they are not Golgi bodies, and did not colocalize with the hexyl rhodamine B stain, suggesting that they are not mitochondria (Supplemental Fig. S3, D–F). Because RDR6 was shown to interact with SGS3 and colocalize with SGS3 in similar punctae (Kumakura et al., 2009), we attempted to also determine the subcellular localization of RDR1. We expressed the *RDR1*:*GFP* transgene under the control of the native promoter, and transgenic *rdr1-2 cer7-1* plants carrying *ProRDR1*:*RDR1*:*GFP* were wax deficient like the *cer7-1* mutant, indicating that the RDR1:GFP fusion protein was functional. However, we were unable to detect strong fluorescent signal by confocal microscopy in any of the complemented lines. Low RDR1:GFP expression levels may be due to the weak RDR1 promoter.

RDR1 and SGS3 Are Involved in the Regulation of *CER3* Expression in Developing Inflorescence Stems

Our suppressor screen resulted in the identification of several alleles of *RDR1* and *SGS3*, suggesting that an RNA-based regulatory mechanism, possibly involving small RNAs, controls *CER3* expression during cuticular wax deposition in developing inflorescence stems. During development, cuticular wax is synthesized predominantly at the top of the stem, where the stem is actively elongating, and waxes are deposited evenly along the stem (Suh et al., 2005). This requires higher expression of wax biosynthetic genes, including *CER3*, at the top of the stem than at the stem base.

To determine if *CER3* transcription is developmentally regulated in Arabidopsis inflorescence stems, and to investigate whether RNA silencing is involved in modulating *CER3* expression, we monitored *CER3* transcript levels in elongating stems by real-time PCR. As expected, *CER3* transcript levels were considerably greater at the stem top than at the base of wild-type stems (Fig. 7). As shown previously, *cer7-1* mutant plants displayed reduced *CER3* transcript accumulation (Hooker et al., 2007) that did not significantly differ between the stem top and stem base. By contrast, introduction of the *rdr1-2* or *sgs3-15* mutation in the *cer7-1* background resulted in a major surge in *CER3*

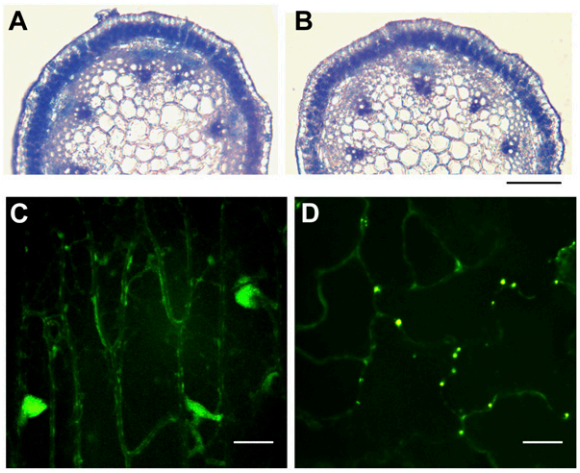

Figure 6. Expression of *RDR1* and *SGS3*. A and B, Tissue-specific expression of *ProRDR1:GUS* and *ProSGS3:GUS* in Arabidopsis stems. Stems of 4-week-old transgenic plants expressing *ProRDR1:GUS* (A) and *ProSGS3:GUS* (B) were stained for *GUS* activity. Cross-sections from the top 3 cm of the stem are shown. Bar = 0.1 mm. C and D, Localization of *SGS3* by confocal microscopy. In stems, SGS3:YFP is localized to the ER (C). In leaves, SGS3:YFP is localized to the cytoplasm and to punctae (D). Images are Z-projections of confocal stacks. Bars = 10 μm.

transcript accumulation, with the *CER3* transcript reaching severalfold greater levels than those detected in the wild-type stem top and stem base (Fig. 7). These data indicate that RDR1 and SGS3, implicated in small RNA biogenesis, are necessary for the down-regulation of *CER3* during the development of Arabidopsis inflorescence stems.

DISCUSSION

We previously proposed a novel mechanism of regulating cuticular wax biosynthesis in developing Arabidopsis inflorescence stems, which involves the CER7 exosomal RNase (Hooker et al., 2007). We hypothesized that CER7 controls the transcription of *CER3*, a key wax biosynthetic gene, via the degradation of an mRNA encoding a negative regulator of *CER3*. To test this model, we expressed the *CER3* transgene in the *cer7-3* mutant using the epidermis-specific *CER6* promoter, which is not affected by the same negative regulator as *CER3*, and successfully complemented the *cer7-3* stem wax phenotype.

To identify the proposed negative regulator and other factors required for CER7-mediated control of *CER3* expression, we performed a screen for suppressors of *cer7-1*, which restore *cer7*-related stem wax deficiency to wild-type wax levels. We isolated four classes of suppressors designated *war1* to *war4*. In this study, we characterized *war3* and *war4* and the genes disrupted by these mutations. *WAR3* encodes RDR1, one of the six RDR proteins described in Arabidopsis. RDR proteins have been found in diverse eukaryotes and are considered to be core members of the RNA-silencing machinery. They catalyze the conversion of a single-stranded RNA template into dsRNA, which serves as a substrate for DICER-like enzymes in the production of a type of small RNAs termed siRNAs. It is well documented that RDR2 and RDR6 participate in siRNA-mediated gene silencing in Arabidopsis (Peragine et al., 2004; Vazquez et al., 2004; Xie and Qi, 2008), but evidence for such a role for RDR1 is currently lacking, as it has only been reported to be involved in antiviral defense by promoting the turnover of viral RNAs in infected plants (Yu et al., 2003). Moreover, Yu et al. (2003) reported that RDR1 expression in leaves is only induced upon viral infection; however, we observed that RDR1 was constitutively expressed in most tissues at varying levels, consistent with expression patterns from the At-TAX tiling microarray experiments (Laubinger et al., 2008).

Map-based cloning of *WAR4* revealed that it encodes SGS3, a plant-specific protein suggested to bind

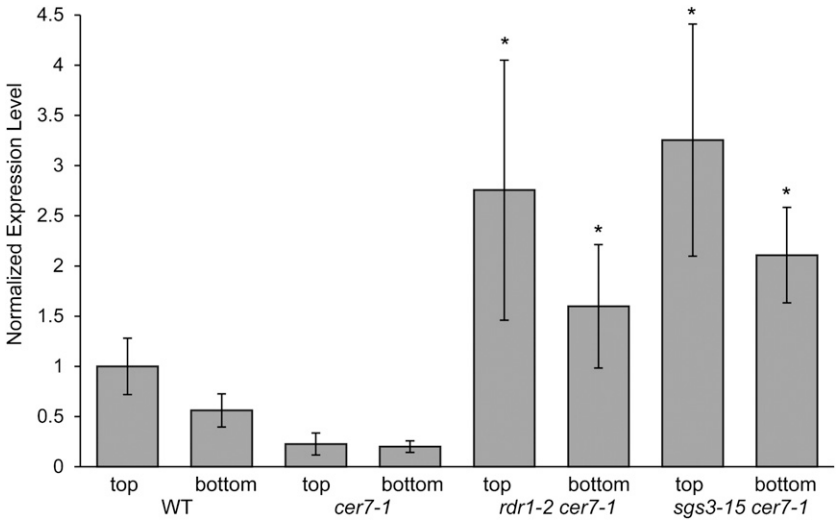

Figure 7. *CER3* expression levels in the top 3 cm and the bottom 3 cm of a 10-cm stem as measured by quantitative RT-PCR. *ACTIN2* was used as an internal control, and control samples were normalized to 1. Values represent means ± SD (n = 4), and statistically significant differences ($P < 0.05$) are indicated by asterisks. WT, Wild type.

and stabilize RNA template to initiate RDR-catalyzed dsRNA synthesis. SGS3 is essential for the synthesis of dsRNA in transgene silencing, virus silencing, and the synthesis of trans-acting siRNAs involved in the regulation of gene expression during normal plant development (Peragine et al., 2004), and it has been shown to directly interact with RDR6 in cytoplasmic punctae (Kumakura et al., 2009).

The identification of RDR1 and SGS3 in our screen for the *cer7-1* suppressors demonstrates that, in addition to RDR6, RDR1 function also requires the participation of SGS3. Furthermore, even though RDR1 has not been reported to be involved in endogenous gene silencing, based on our results it seems reasonable to speculate that RDR1 and SGS3 are involved in the production of an as yet uncharacterized small RNA species that directly or indirectly mediates transcriptional gene silencing of *CER3* to control wax deposition over the length of the stem. At the top of the stem where the stem is actively growing, wax biosynthetic genes are highly expressed (Suh et al., 2005). Conversely, at the base of the stem where growth has terminated, the expression of wax biosynthetic genes is reduced. As expected, in the wild type, we found higher levels of the *CER3* transcript in the stem top compared with the stem base (Fig. 7). In the *cer7-1* mutant, *CER3* expression is significantly decreased, with *CER3* transcript levels being similarly low in both the top and bottom of the stem, which results in the wax-deficient phenotype. In contrast to the *cer7-1* mutant, *CER3* transcript levels in *rdr1-2 cer7-1* and *sgs3-15 cer7-1* double mutants are considerably higher in both the top and the stem base than *CER3* levels detected in the wild type (Fig. 7), resulting in the restoration of stem wax loads.

The simplest model that integrates all our findings is presented in Figure 8. Small RNA precursors are known targets of the exosomal RNA ribonucleases (Chekanova et al., 2007). We hypothesize that in the wild-type stem tops, where *CER7* is highly expressed (Supplemental Fig. S4) and the CER7 activity is presumably high, this exosomal RNase degrades a precursor of a small RNA species that acts as a repressor of *CER3* expression. This results in enhanced *CER3* transcription and wax production via the decarbonylation pathway. *CER7* expression progressively decreases from the top toward the base of the stem (Supplemental Fig. S4), causing a gradual increase in small RNA accumulation. This is associated with the down-regulation of *CER3* expression in the epidermal cells and the cessation of wax production at the stem base. In the *cer7* mutant, where the CER7 exosomal subunit is not functional, the buildup of small RNAs causes *CER3* silencing and stem wax deficiency. The biogenesis of small RNA precursors involved in the silencing of *CER3* requires RDR1 and SGS3 activities. In the absence of RDR1 or SGS3 in the *rdr1 cer7* or *sgs3 cer7* double mutant, respectively, the small RNA species responsible for *CER3* repression will not be generated, abolishing the need for CER7 in wax biosynthesis.

In an attempt to verify this model and identify the potential small RNA species that represses *CER3* expression, we identified 33 small RNAs that map to the region upstream of *CER3* (Arabidopsis Small RNA Project 2010 [http://asrp.cgrb.oregonstate.edu/]). However, none of these RNAs map to the fragment of the

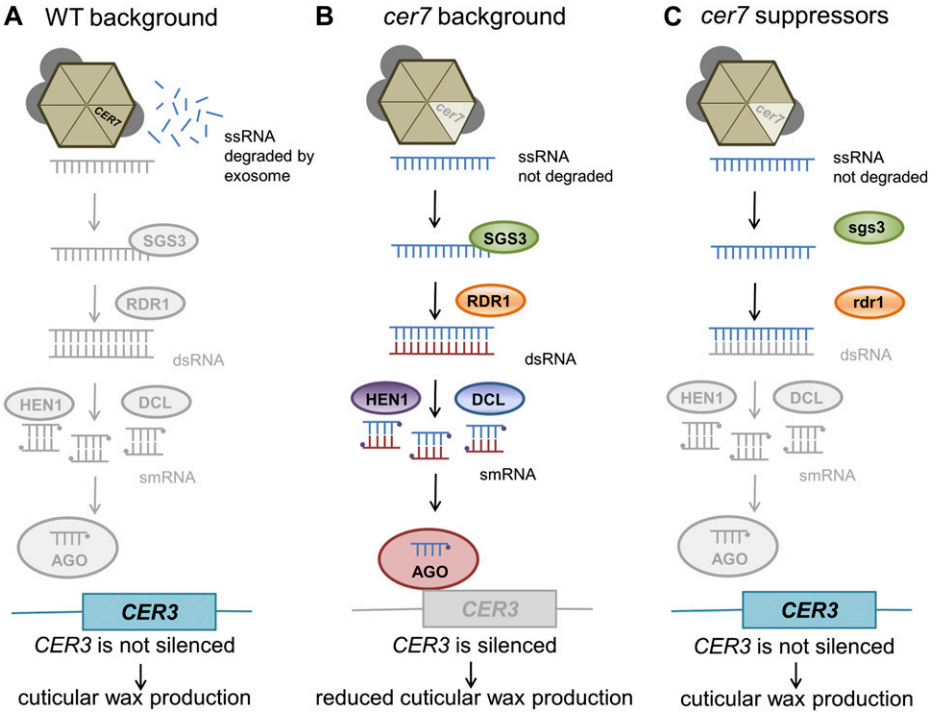

Figure 8. Model illustrating the roles of RDR1 and SGS3, components of RNA silencing, in regulating cuticular wax biosynthesis at the top of the stem. A, In the wild type (WT), the precursor of the small RNA (smRNA) that regulates the expression of *CER3* is degraded by CER7; therefore, *CER3* is expressed and cuticular wax production ensues. B, In the *cer7* mutant, the smRNA precursor is not degraded and is used for the production of a smRNA species by a pathway that involves RDR1 and SGS3. smRNA functions to silence *CER3*, leading to decreased cuticular wax biosynthesis. C, In either *rdr1* or *sgs3*, suppressors of *cer7*, the smRNA species responsible for *CER3* silencing will not be synthesized, resulting in *CER3* expression and wax production in the absence of CER7 activity. *DCL*, *DICER-LIKE*; *HEN1*, *HUA ENHANCER1*; *AGO*, *ARGONAUTE*.

CER3 promoter that was used in our previous experiments to demonstrate that CER7 is required for transcription of the *CER3* gene during stem wax deposition (Hooker et al., 2007). This suggests that the regulation of *CER3* expression by small RNAs may be indirect and could involve another component, perhaps a positive regulator of *CER3* transcription, which is controlled by posttranscriptional gene silencing. In this scenario, in wild-type stem tops, the precursor of the small RNA repressor may be degraded by CER7, allowing the putative positive regulator to activate *CER3* transcription. At the bottom of the stem, where the *CER7* activity is lower, the small RNA repressor may silence the positive regulator of *CER3*, causing the down-regulation of *CER3* expression. In the *cer7* mutant, there may be a large accumulation of the small RNA repressor throughout the stem, silencing a positive regulator of *CER3* and resulting in very low levels of *CER3* transcription. In the *rdr1 cer7* and *sgs3 cer7* double mutants that lack the small RNA repressor, the putative positive regulator of *CER3* would be continuously expressed, causing high levels of *CER3* transcription and wax biosynthesis.

CONCLUSION

We have uncovered a novel mechanism of regulating cuticular wax biosynthesis during stem elongation, which involves the exosome and RNA-mediated gene silencing. Such an intricate system of regulation may be utilized by the plant to control metabolism during cuticle development, as a great amount of energy is expended by epidermal cells to generate cuticular lipids. RNA silencing of *CER3* expression requires SGS3 and RDR1, providing evidence that RDR1 plays a role in gene regulation in addition to its role in antiviral defense. Identifying other components involved in this process, the RNA species responsible, and its target are important objectives for future research.

MATERIALS AND METHODS

Plant Material and Growth Conditions

Arabidopsis (*Arabidopsis thaliana*) *cer7-1 sti* and *cer7-3* are in the L*er* genetic background and the Columbia-0 genetic background, respectively. T-DNA insertion lines *rdr1-1*, *rdr1-5* (SALK_109922), *rdr1-6* (SALK_112300), *rdr1-7* (SALK_125022), *rdr1-8* (SALK_007638), *sgs3-13* (SALK_039005), and *sgs3-14* (SALK_001394) are in the Columbia-0 genetic background and were obtained from the Arabidopsis Biological Resource Center (www.arabidopsis.org). Seeds were germinated on AT-agar plates (Somerville and Ogren, 1982) for 7 to 10 d and transplanted to soil (Sunshine Mix 4; SunGro). All plants were grown at 20°C under continuous light (90–110 μE m^{-2} s^{-1} photosynthetically active radiation) in an environmental chamber.

Molecular Complementation of *cer7* with the *CER3* Transgene

The 1,899-bp CER3 coding region was excised from the plasmid pESC-TRP:ProGAL1:CER3 (P. Lam, unpublished data) using *Bam*HI and *Nhe*I. This fragment was cloned into the plasmid pBluescriptII:ProCER6 (P. Lam, unpublished data) into the corresponding restriction enzyme sites to generate pBluescriptII:ProCER6:CER3. The ProCER6-CER3 fragment was then excised using *Xho*I and *Sst*I and cloned into pRD400 (Datla et al., 1992), which was excised with *Sal*I and *Sst*I (*Sal*I and *Xho*I form compatible ends). The resulting plasmid, pRD400:ProCER6:CER3, was transformed into *Agrobacterium tumefaciens* strain GV3101, pMP90 (Koncz and Schell, 1986), via electroporation. *cer7-3* plants were transformed using the floral dip method (Clough and Bent, 1998).

Mutagenesis of *cer7-1 sti*

Approximately 12,000 *cer7-1 sti* seeds were soaked in a solution of 0.1 M Na_3PO_4, 5% dimethyl sulfoxide, and 100 mM ethyl methanesulfonate for 5 h. After mutagenesis, the seeds were washed twice with 100 mM $Na_2S_2O_3$ and then twice with distilled water for 15 min per wash. Seeds were allowed to dry overnight before planting directly in soil in 64 total pots. Plants were grown until maturity, and M2 seeds were harvested collectively from each pot, yielding 64 batches. In the primary screen, M2 seeds from each of the 64 batches were grown up and scored for a waxy stem phenotype. Plants that did not have a waxy phenotype were discarded. Those plants that were waxy were grown to maturity, and seeds were harvested individually. These plants were then subjected to a secondary screen to confirm that they did have a waxy stem, the *sti* trichome, and that the *cer7-1* mutation was still present.

Genotyping

DNA was extracted according to Berendzen et al. (2005). To genotype *cer7-1*, derived cleaved-amplified polymorphic sequence primers cer7-1_*Afl*II-F and cer7-1_*Afl*II-R were used to amplify a 210-bp fragment. The PCR product was then digested with *Afl*II and run on a 1.5% agarose gel. The mutation in *cer7-1* allows for cleavage of the PCR product after *Afl*II digestion, resulting in 185- and 25-bp products. T-DNA insertion lines were genotyped using LBb1.3 and gene-specific primers as listed in Supplemental Table S3.

Cuticular Wax Extraction and Analysis

Cuticular waxes were extracted from 4- to 6-week-old Arabidopsis stems. Stems were immersed for 30 s in chloroform containing 10 μg of *n*-tetracosane, which was used as an internal standard. After extraction, samples were blown down under a gentle stream of nitrogen and redissolved in 10 μL of *N,O*-bis(trimethylsilyl) trifluoroacetamide (Sigma) and 10 μL of pyridine (Fluka). Samples were derivatized for 90 min at 80°C. After derivatization, excess *N,O*-bis(trimethylsilyl) trifluoroacetamide and pyridine were removed by blowing down under nitrogen, and samples were dissolved in 30 μL of chloroform. Gas-liquid chromatography was performed in the samples using a HP 6890 series gas chromatograph equipped with flame ionization detection and a 30m HP-1 column with helium as the carrier gas. Gas chromatography was carried out with temperature-programmed on-column injection and oven temperature set at 50°C for 2 min, raised by 40°C min^{-1} to 200°C, held for 2 min at 200°C, raised by 3°C min^{-1} to 320°C, and held for 30 min at 320°C.

Quantification of wax loads was determined by comparing the flame ionization detector peak areas with the internal standard. Stem surface area was calculated by photographing stems prior to wax extraction, measuring the number of pixels, converting them to cm^2, and multiplying by π.

Quantitative RT-PCR

RNA was extracted from plant tissue using TRIzol (Invitrogen) as per the manufacturer's protocol. RNA quantification was performed using a NanoDrop 8000 (Thermo Scientific). Five hundred nanograms of total RNA was treated with DNaseI (Fermentas) and then used for first-strand cDNA synthesis using iScript RT supermix (Bio-Rad). Quantitative RT-PCR was performed using gene-specific primer sets from Supplemental Table S3, in 20-μL reactions using iQ SYBR Green supermix (Bio-Rad), and run on the iQ5 real-time PCR detection system (Bio-Rad). Data were analyzed using the method of Pfaffl (2001), and control samples were normalized to 1. Statistical significance was measured with Student's *t* test.

Positional Cloning of Suppressor Lines

To map the positions of suppressor lines, each suppressor line was crossed to *cer7-3* and grown to the F2 generation. DNA from leaves was collected on FTA cards (Whatman), and 30 to 40 plants with the wild-type waxy stem

phenotype (plants homozygous for the suppressor mutation) were subjected to PCR using simple sequence length polymorphism markers to determine linkage. To further pinpoint the location of each suppressor locus, over 1,000 plants were screened with simple sequence length polymorphism markers until a narrow interval was found.

Molecular Complementation of Suppressor Lines, and Subcellular Localization of RDR1 and SGS3

A 5,252-bp DNA fragment containing 1,754 bp of the upstream region of *RDR1* and the coding region minus the stop codon was amplified from wild-type Columbia-0 plants with primers RDR1p-attB1 and RDR1-attB2_noSTOP using Phusion polymerase (Finnzymes). Gateway adapters were added using the adapter protocol (Invitrogen). This 5,252-bp fragment was cloned into pDONR221 using BP Clonase II (Invitrogen) to create pDONR221:ProRDR1:RDR1ΔSTOP and was sequenced to confirm that no mutations were introduced during PCR. The fragment was then recombined into the destination vector pGWB4 (Nakagawa et al., 2007) using LR Clonase II (Invitrogen) to generate pGWB4:ProRDR1:RDR1:GFP.

To generate SGS3:YFP for subcellular localization analysis, the coding sequence of *SGS3* (*At5g23570*) was obtained from leaf cDNA using primers SGS3-attB1 and SGS3-attB2_noSTOP with Phusion polymerase (Finnzymes). The PCR product was introduced into the pDONR207 entry vector using BP Clonase II (Invitrogen). Sequencing was performed to confirm error-free inserts, which were then transferred to the binary vectors pEarleyGate104 (Earley et al., 2006) using LR Clonase II (Invitrogen).

These constructs were introduced into *rdr1-2 cer7-1* and *sgs3-15 cer7-1* plants via *Agrobacterium*-mediated transformation as described above.

Spinning-disk confocal microscopy was performed on a Perkin-Elmer Ultraview VoX Spinning Disk Confocal Microscope mounted on a Leica DMI6000 inverted microscope. GFP and YFP were detected using a 488-nm laser and 528/38-nm emission filters. For ER staining, stems and leaves of transgenic *sgs3-15 cer7-1* plants expressing SGS3-YFP were immersed in hexyl rhodamine B solution (1.6 μM) for 10 to 30 min. Hexyl rhodamine B was excited with a 561-nm laser line and a 600-nm long-pass emission filter. Acquired images were processed using Volocity (Improvision) and ImageJ.

RDR1 and *SGS3* Promoter:GUS Fusions, and GUS Activity Assay

To generate *ProRDR1:GUS*, a 1,754-bp region upstream of the *RDR1* initiation codon was amplified from genomic DNA using the primers RDR1pro_*Eco*RI-F and RDR1_*Xba*I-R with Phusion polymerase (Finnzymes). The PCR product was digested with *Eco*RI and *Xba*I and cloned into the corresponding restriction enzyme sites of pBluescript II SK+ (Stratagene). After confirmation that no errors were induced from PCR, the *ProRDR1* region was excised using *Sal*I and *Bam*HI and cloned into the corresponding sites of pBI101 (Clontech) to generate *pBI101:ProRDR1:GUS*. To generate *ProSGS3:GUS*, a 2,177-bp-long region containing 2,141 bp immediately upstream of the *SGS3* translation start site and 36 bp downstream of the *SGS3* translation start site was amplified from genomic DNA using gene-specific primers SGS3pro-attB1 and SGS3pro-attB2 with Phusion polymerase (Finnzymes). The obtained fragment was introduced to pDONR207 entry vector, sequenced to confirm accuracy, and transferred into the pMDC163 destination vector.

Stems from transgenic plants containing the *ProRDR1:GUS* and *ProSGS3:GUS* constructs were removed and immersed in GUS staining buffer containing 0.5 mM potassium ferricyanide, 0.5 mM potassium ferrocyanide, 100 mM Na_2HPO_4, 100 mM NaH_2PO_4, 0.2% Triton X-100, and 1 mM 5-bromo-4-chloro-3-indolyl-β-D-glucuronide for 1 to 2 h at 37°C. Stems were then cleared of chlorophyll by overnight incubation in 75% ethanol. Stained and cleared samples were examined by compound light microscopy.

Sequence data from this article can be obtained from the Arabidopsis Genome Initiative database under the following accession numbers: *CER7* (*At3g60500*), *CER3* (*At5g57800*), *RDR1* (*At1g14790*), and *SGS3* (*At5g23570*).

Supplemental Data

The following materials are available in the online version of this article.

Supplemental Figure S1. Wax levels are restored in *rdr1-7 cer7-3* and *sgs3-13 cer7-3* double mutants.

Supplemental Figure S2. The *RDR1* and *SGS3* transgenes can complement *war3-1 cer7-1* and *war4-1 cer7-1*, respectively.

Supplemental Figure S3. Colocalization of the SGS3:YFP-labeled network and the ER network stained by hexyl rhodamine B.

Supplemental Figure S4. Quantitative RT-PCR of *CER7* expression levels in the top 3 cm and the bottom 3 cm of a 10-cm stem as well as the epidermis.

Supplemental Table S1. Nomenclature and description of the *rdr1* alleles.

Supplemental Table S2. Nomenclature and description of the *sgs3* alleles.

Supplemental Table S3. Primers used in this study.

ACKNOWLEDGMENTS

We thank the Salk Institute for Genomic Analysis Laboratory for providing sequence-indexed Arabidopsis T-DNA insertion mutants, the Bioimaging Facility at the University of British Columbia for help with microscopy, Jonathan Griffiths and Tegan Haslam for helpful discussions and critical evaluation of the manuscript, and Donald Yung for technical assistance.

Received May 2, 2012; accepted June 11, 2012; published June 11, 2012.

LITERATURE CITED

Aharoni A, Dixit S, Jetter R, Thoenes E, van Arkel G, Pereira A (2004) The SHINE clade of AP2 domain transcription factors activates wax biosynthesis, alters cuticle properties, and confers drought tolerance when overexpressed in *Arabidopsis*. Plant Cell **16:** 2463–2480

Alonso JM, Stepanova AN, Leisse TJ, Kim CJ, Chen H, Shinn P, Stevenson DK, Zimmerman J, Barajas P, Cheuk R, et al (2003) Genome-wide insertional mutagenesis of Arabidopsis thaliana. Science **301:** 653–657

Bach L, Michaelson LV, Haslam R, Bellec Y, Gissot L, Marion J, Da Costa M, Boutin J-P, Miquel M, Tellier F, et al (2008) The very-long-chain hydroxy fatty acyl-CoA dehydratase PASTICCINO2 is essential and limiting for plant development. Proc Natl Acad Sci USA **105:** 14727–14731

Barthlott W, Neinhuis C (1997) Purity of the sacred lotus, or escape from contamination in biological surfaces. Planta **202:** 1–8

Beaudoin F, Wu X, Li F, Haslam RP, Markham JE, Zheng H, Napier JA, Kunst L (2009) Functional characterization of the Arabidopsis β-ketoacyl-coenzyme A reductase candidates of the fatty acid elongase. Plant Physiol **150:** 1174–1191

Berendzen K, Searle I, Ravenscroft D, Koncz C, Batschauer A, Coupland G, Somssich IE, Ulker B (2005) A rapid and versatile combined DNA/RNA extraction protocol and its application to the analysis of a novel DNA marker set polymorphic between Arabidopsis thaliana ecotypes Col-0 and Landsberg erecta. Plant Methods **1:** 4

Broun P, Poindexter P, Osborne E, Jiang C-Z, Riechmann JL (2004) WIN1, a transcriptional activator of epidermal wax accumulation in Arabidopsis. Proc Natl Acad Sci USA **101:** 4706–4711

Chekanova JA, Gregory BD, Reverdatto SV, Chen H, Kumar R, Hooker T, Yazaki J, Li P, Skiba N, Peng Q, et al (2007) Genome-wide high-resolution mapping of exosome substrates reveals hidden features in the Arabidopsis transcriptome. Cell **131:** 1340–1353

Clough SJ, Bent AF (1998) Floral dip: a simplified method for Agrobacterium-mediated transformation of Arabidopsis thaliana. Plant J **16:** 735–743

Dalmay T, Hamilton A, Rudd S, Angell S, Baulcombe DC (2000) An RNA-dependent RNA polymerase gene in Arabidopsis is required for post-transcriptional gene silencing mediated by a transgene but not by a virus. Cell **101:** 543–553

Datla RSS, Hammerlindl JK, Panchuk B, Pelcher LE, Keller W (1992) Modified binary plant transformation vectors with the wild-type gene encoding NPTII. Gene **122:** 383–384

Earley KW, Haag JR, Pontes O, Opper K, Juehne T, Song K, Pikaard CS (2006) Gateway-compatible vectors for plant functional genomics and proteomics. Plant J **45:** 616–629

Eigenbrode SD, Espelie KE (1995) Effects of plant epicuticular lipids on insect herbivores. Annu Rev Entomol **40:** 171–194

Elmayan T, Adenot X, Gissot L, Lauressergues D, Gy I, Vaucheret H (2009) A neomorphic sgs3 allele stabilizing miRNA cleavage products reveals that SGS3 acts as a homodimer. FEBS J **276:** 835–844

Glick E, Zrachya A, Levy Y, Mett A, Gidoni D, Belausov E, Citovsky V, Gafni Y (2008) Interaction with host SGS3 is required for suppression of RNA silencing by tomato yellow leaf curl virus V2 protein. Proc Natl Acad Sci USA **105:** 157–161

Greer S, Wen M, Bird D, Wu X, Samuels L, Kunst L, Jetter R (2007) The cytochrome P450 enzyme CYP96A15 is the midchain alkane hydroxylase responsible for formation of secondary alcohols and ketones in stem cuticular wax of Arabidopsis. Plant Physiol **145:** 653–667

Hooker TS, Lam P, Zheng H, Kunst L (2007) A core subunit of the RNA-processing/degrading exosome specifically influences cuticular wax biosynthesis in *Arabidopsis*. Plant Cell **19:** 904–913

Ilgenfritz H, Bouyer D, Schnittger A, Mathur J, Kirik V, Schwab B, Chua N-H, Jürgens G, Hülskamp M (2003) The Arabidopsis STICHEL gene is a regulator of trichome branch number and encodes a novel protein. Plant Physiol **131:** 643–655

Jetter R, Kunst L, Samuels L (2006) Composition of plant cuticular waxes. *In* M Riederer, C Muller, eds, Biology of the Plant Cuticle, Vol 23. Blackwell Publishing, Oxford, pp 145–181

Kannangara R, Branigan C, Liu Y, Penfield T, Rao V, Mouille G, Höfte H, Pauly M, Riechmann JL, Broun P (2007) The transcription factor WIN1/SHN1 regulates cutin biosynthesis in *Arabidopsis thaliana*. Plant Cell **19:** 1278–1294

Koncz C, Schell J (1986) The promoter of TL-DNA gene 5 controls the tissue-specific expression of chimaeric genes carried by a novel type of Agrobacterium binary vector. Mol Gen Genet **204:** 383–396

Kumakura N, Takeda A, Fujioka Y, Motose H, Takano R, Watanabe Y (2009) SGS3 and RDR6 interact and colocalize in cytoplasmic SGS3/RDR6-bodies. FEBS Lett **583:** 1261–1266

Laubinger S, Zeller G, Henz SR, Sachsenberg T, Widmer CK, Naouar N, Vuylsteke M, Schölkopf B, Rätsch G, Weigel D (2008) At-TAX: a whole genome tiling array resource for developmental expression analysis and transcript identification in *Arabidopsis thaliana*. Genome Biol **9:** R112

Li F, Wu X, Lam P, Bird D, Zheng H, Samuels L, Jetter R, Kunst L (2008) Identification of the wax ester synthase/acyl-coenzyme A:diacylglycerol acyltransferase WSD1 required for stem wax ester biosynthesis in Arabidopsis. Plant Physiol **148:** 97–107

Millar AA, Clemens S, Zachgo S, Giblin EM, Taylor DC, Kunst L (1999) CUT1, an *Arabidopsis* gene required for cuticular wax biosynthesis and pollen fertility, encodes a very-long-chain fatty acid condensing enzyme. Plant Cell **11:** 825–838

Mourrain P, Béclin C, Elmayan T, Feuerbach F, Godon C, Morel J-B, Jouette D, Lacombe A-M, Nikic S, Picault N, et al (2000) Arabidopsis SGS2 and SGS3 genes are required for posttranscriptional gene silencing and natural virus resistance. Cell **101:** 533–542

Nakagawa T, Kurose T, Hino T, Tanaka K, Kawamukai M, Niwa Y, Toyooka K, Matsuoka K, Jinbo T, Kimura T (2007) Development of series of Gateway binary vectors, pGWBs, for realizing efficient construction of fusion genes for plant transformation. J Biosci Bioeng **104:** 34–41

Nawrath C (2006) Unraveling the complex network of cuticular structure and function. Curr Opin Plant Biol **9:** 281–287

Peragine A, Yoshikawa M, Wu G, Albrecht HL, Poethig RS (2004) SGS3 and SGS2/SDE1/RDR6 are required for juvenile development and the production of trans-acting siRNAs in Arabidopsis. Genes Dev **18:** 2368–2379

Pfaffl MW (2001) A new mathematical model for relative quantification in real-time RT-PCR. Nucleic Acids Res **29:** e45

Pollard M, Beisson F, Li Y, Ohlrogge JB (2008) Building lipid barriers: biosynthesis of cutin and suberin. Trends Plant Sci **13:** 236–246

Raffaele S, Vailleau F, Léger A, Joubès J, Miersch O, Huard C, Blée E, Mongrand S, Domergue F, Roby D (2008) A MYB transcription factor regulates very-long-chain fatty acid biosynthesis for activation of the hypersensitive cell death response in *Arabidopsis*. Plant Cell **20:** 752–767

Reicosky DA, Hanover JW (1978) Physiological effects of surface waxes. I. Light reflectance for glaucous and nonglaucous *Picea pungens*. Plant Physiol **62:** 101–104

Riederer M (2006) Introduction: biology of the plant cuticle. *In* M Riederer, C Muller, eds, Biology of the Plant Cuticle, Vol 23. Blackwell Publishing, Oxford, pp 1–10

Riederer M, Schreiber L (2001) Protecting against water loss: analysis of the barrier properties of plant cuticles. J Exp Bot **52:** 2023–2032

Rowland O, Lee R, Franke R, Schreiber L, Kunst L (2007) The CER3 wax biosynthetic gene from Arabidopsis thaliana is allelic to WAX2/YRE/FLP1. FEBS Lett **581:** 3538–3544

Rowland O, Zheng H, Hepworth SR, Lam P, Jetter R, Kunst L (2006) CER4 encodes an alcohol-forming fatty acyl-coenzyme A reductase involved in cuticular wax production in Arabidopsis. Plant Physiol **142:** 866–877

Samuels L, Kunst L, Jetter R (2008) Sealing plant surfaces: cuticular wax formation by epidermal cells. Annu Rev Plant Biol **59:** 683–707

Seo PJ, Lee SB, Suh MC, Park M-J, Go YS, Park C-M (2011) The MYB96 transcription factor regulates cuticular wax biosynthesis under drought conditions in *Arabidopsis*. Plant Cell **23:** 1138–1152

Sieber P, Schorderet M, Ryser U, Buchala A, Kolattukudy P, Métraux J-P, Nawrath C (2000) Transgenic *Arabidopsis* plants expressing a fungal cutinase show alterations in the structure and properties of the cuticle and postgenital organ fusions. Plant Cell **12:** 721–738

Somerville CR, Ogren WL (1982) Isolation of photorespiratory mutants of Arabidopsis. *In* Methods in Chloroplast Molecular Biology. Elsevier, New York, pp 129–139

Suh MC, Samuels AL, Jetter R, Kunst L, Pollard M, Ohlrogge J, Beisson F (2005) Cuticular lipid composition, surface structure, and gene expression in Arabidopsis stem epidermis. Plant Physiol **139:** 1649–1665

Vazquez F, Vaucheret H, Rajagopalan R, Lepers C, Gasciolli V, Mallory AC, Hilbert J-L, Bartel DP, Crété P (2004) Endogenous trans-acting siRNAs regulate the accumulation of Arabidopsis mRNAs. Mol Cell **16:** 69–79

Wang Z-Y, Xiong L, Li W, Zhu J-K, Zhu J (2011) The plant cuticle is required for osmotic stress regulation of abscisic acid biosynthesis and osmotic stress tolerance in *Arabidopsis*. Plant Cell **23:** 1971–1984

Wu R, Li S, He S, Wassmann F, Yu C, Qin G, Schreiber L, Qu L-J, Gu H (2011) CFL1, a WW domain protein, regulates cuticle development by modulating the function of HDG1, a class IV homeodomain transcription factor, in rice and *Arabidopsis*. Plant Cell **23:** 3392–3411

Xie Z, Johansen LK, Gustafson AM, Kasschau KD, Lellis AD, Zilberman D, Jacobsen SE, Carrington JC (2004) Genetic and functional diversification of small RNA pathways in plants. PLoS Biol **2:** E104

Xie Z, Qi X (2008) Diverse small RNA-directed silencing pathways in plants. Biochim Biophys Acta **1779:** 720–724

Yoshikawa M, Peragine A, Park MY, Poethig RS (2005) A pathway for the biogenesis of trans-acting siRNAs in Arabidopsis. Genes Dev **19:** 2164–2175

Yu D, Fan B, MacFarlane SA, Chen Z (2003) Analysis of the involvement of an inducible Arabidopsis RNA-dependent RNA polymerase in antiviral defense. Mol Plant Microbe Interact **16:** 206–216

Zheng H, Rowland O, Kunst L (2005) Disruptions of the *Arabidopsis* enoyl-CoA reductase gene reveal an essential role for very-long-chain fatty acid synthesis in cell expansion during plant morphogenesis. Plant Cell **17:** 1467–1481